

EPR and modelling studies of hydrogen-abstraction reactions relevant to polyolefin cross-linking and grafting chemistry †

Susana Camara,^a Bruce C. Gilbert,^{*a} Robert J. Meier,^b Martin van Duin^b and Adrian C. Whitwood^a

^a University of York, Department of Chemistry, Heslington, York, UK YO10 5DD.

E-mail: bcg1@york.ac.uk. E-mail: acw1@york.ac.uk

^b DSM Research, 6160 MD Geleen, Netherlands. E-mail: Martin.Duin-van@dsm.com.

E-mail: r.meier@wxs.nl

Received 23rd December 2002, Accepted 12th February 2003

First published as an Advance Article on the web 10th March 2002

EPR spectroscopy has been employed to study directly the selectivity of hydrogen-atom abstraction by some alkoxy radicals from a variety of linear and branched alkanes, as well as linear alkenes, chosen as models for low molecular-weight polyolefin cross-linking systems. *In situ* thermal and photolytic approaches, as well as spin-trapping, have been employed to provide information relating to an accessible temperature range of 233–453 K, in part to mimic conditions relevant to melt processing of polyolefins. Rate constants (in the range $3 \times 10^3 - 3.7 \times 10^5 \text{ dm}^3 \text{ mol}^{-1} \text{ s}^{-1}$ per hydrogen) have been determined for C–H abstraction at room temperature. Radical selectivity is largely governed by enthalpic effects (modelled *via* bond dissociation energy calculations and kinetic analysis). Direct evidence has been obtained for lack of reactivity, as a result of unfavourable steric interactions, for the secondary and tertiary C–H bonds in 2,4-dimethylpentane and 2,4,6-trimethylheptane, models for polypropylene. This has been rationalized *via* free-energy calculations using DFT.

1. Introduction

EPR Spectroscopy provides a unique method for determining the sites of attack of reactive free-radicals (*e.g.* alkoxy radicals from peroxides) on organic substrates and biomolecules. Under certain circumstances, it is possible to estimate absolute radical concentrations and, from hyperfine splittings, to characterise individual radicals. This may then lead to the determination of the selectivity towards radical attack at different sites, which itself may reflect the interplay of a number of potential contributions: these include thermochemical effects (radical stability and influences of bond dissociation energy), as well as steric, stereo-electronic and polar effects.¹ Areas of particular interest relevant to our work include the factors influencing the selectivity towards C–H abstraction in ester molecules (used as models for lubricants²), and biomolecules, including mono- and polysaccharides.³ These factors also govern the reactions and applications of such species in antioxidant processes and, in some cases, in synthetic schemes.

The research reported here reflects our interest in cross-linking and grafting reactions in polymers as accomplished by the use of peroxides. Relative abstraction rates for different types of C–H bonds will have an impact on the structures formed, and therefore on the properties of the polymeric material finally obtained. It is, however, by no means clear that the kinetics of radical formation by hydrogen-abstraction from low molecular weight molecules, in our case more specifically alkanes, directly applies to polymers under processing conditions. Therefore we have first utilised EPR spectroscopy to explore and quantify the preferred sites of attack on saturated and unsaturated hydrocarbons containing primary, secondary and tertiary C–H bonds. The compounds were selected to form a set of low

molecular-weight model compounds representing characteristic moieties from polyethylene, polypropylene and ethylene–propylene (co-)polymers. We have employed octane, decane, eicosane (C₂₀H₄₂) and tetracontane (C₄₀H₈₂) as models for polyethylene (PE), 2,4-dimethylpentane and 2,4,6-trimethylheptane as models for polypropylene (PP), and squalane (C₃₀H₆₂) and 2,6,10,14-tetramethylpentadecane as models for ethylene–propylene copolymers (EPM). Because of the presence of unsaturation in commercially produced polymers and the observation of allyl radicals in previous EPR experiments on polyolefins,⁴ we have also investigated some related model compounds, including 4-octene, 5-decene, 1-octadecene and 9-octadecene. Further knowledge obtained from these studies should underpin a more detailed understanding of the behaviour of such polymers in a variety of reactions, including cross-linking and grafting, which are involved in polymer modification in the presence of free-radicals derived, usually thermally, from peroxides.⁵

This approach should provide evidence which is direct and complementary to that obtained *via* indirect approaches. For example, product studies have underpinned the investigation of selectivity of *tert*-butoxyl towards alkanes, data has been compiled by Howard and coworkers⁶ and also reported by Walling and Jacknow.⁷ Other approaches have involved spin-trapping with 2-methyl-2-nitrosopropane (MNP), in which EPR spectroscopy has been used for identifying radical-adducts following alkoxy attack⁸ and the product study–spin-scavenging approach employed by Solomon and co-workers^{9,10} in which the initial radicals are scavenged by reaction with stable nitroxides to give alkoxyamines, characterised by NMR spectroscopy following separation by HPLC. A direct CIDEP/EPR study of the reaction of triplet propanone with linear and branched alkanes has also been reported.¹¹ Whilst the selectivity of attack on C–H bonds generally follows the expected order tertiary > secondary > primary, steric retardation has been proposed for tertiary C–H bonds in *e.g.* 2,4-dimethylpentane^{9,10} and 2,2,4-trimethylpentane¹² and secondary C–H bonds in the former (but contrast the results reported in ref. 11). However, no further rationalization has been provided for this observation.

† Electronic supplementary information (ESI) available: computed 3D structures of the transition states of hydrogen abstraction from 2,4-dimethylpentane by *tert*-butoxyl radical. “1_ry24dmp.pdb”: H-abstraction from the methyl group (to generate a primary radical). “2ry24dmp.pdb”: H-abstraction from the central methylene group (to generate a secondary radical). “3_ry24dmp.pdb”: H-abstraction from the methine group (to generate a tertiary radical). See <http://www.rsc.org/suppdata/ob/b2/b212543a/>

Experiments reported here have involved *in situ* high-resolution EPR spectroscopic studies, using decomposition of di-*tert*-butyl peroxide and 2,5-bis(*tert*-butylperoxy)-2,5-dimethylhexane (Trigonox-101) to generate alkoxy radicals under steady-state conditions. Our approach has employed both thermal and photochemical conditions, for the following reasons. A wide range of substrates can be studied, including low-boiling point hydrocarbons (*e.g.* octane, 4-octene), for which a low temperature photolytic approach is appropriate, and longer-chain alkanes, including eicosane and squalane whose higher boiling points allow study under high-temperature conditions; the latter conditions, typically involving temperatures over 400 K, are similar to those used for polymer processing. In addition, the wide range of temperature (~233–450 K) in principle allows changes in radical conformation and selectivity of radical attack to be studied. It may also be possible to distinguish the reactions of first-formed alkoxy radicals from those of alkyl radicals formed by fragmentation.

Thermolysis experiments with both peroxides (temperature typically *ca.* 450 K) were designed to give a substantial radical flux under the conditions employed so that substrate-derived radicals could be *directly* detected under pseudo steady-state conditions. In order to achieve acceptable signal-to-noise ratios in the EPR spectra, relatively high peroxide–substrate ratios were used (typically 1 : 1). Photolysis experiments, carried out at room temperature and below, involved the use of a high-intensity mercury–xenon arc lamp. *In-situ* EPR observations have been augmented, in some cases, by spin-trapping experiments.

This approach has enabled us to obtain, directly, relative ratios and absolute rate constants for attack of *tert*-butoxyl on a range of linear and branched hydrocarbons including models for polymers. Further structural information and factors governing the selectivity of reaction are reported, along with a kinetic analysis based on calculations of bond-dissociation energies and typical activation parameters reported earlier.⁶ In order to understand the selectivities for hydrogen abstraction as determined from our EPR spectra, we have performed quantum mechanical calculations on hydrogen-abstraction from branched alkanes by *tert*-butoxyl. In a subsequent paper we will discuss an extension of this approach to polymeric samples of related structure.

2. Results and discussion

(a) EPR Spectra of model compounds

(i) **Illustration of typical spectra.** Fig. 1 shows an example of a typical EPR spectrum obtained under (steady-state) *photochemical* conditions from 2,4-dimethylpentane and di-*tert*-butyl peroxide at room temperature (together with a spectrum simulation used to confirm analysis and relative concentrations). The signal to noise ratio was usually found to be moderate (with $[R^{\bullet}]$ typically $\geq 10^{-7}$ mol dm⁻³) and with good resolution ($\Delta H \approx 0.05$ mT). Fig. 2, from eicosane and 2,5-bis(*tert*-butylperoxy)-2,5-dimethylhexane at 443 K, shows a typical spectrum obtained under *thermal* conditions: in most such cases the signal-to-noise ratio was moderate and the lower resolution reflects both this and the need to record under conditions of high modulation and more rapid field scan. Fig. 3 shows a (typical) decay of the steady-state radical concentration: the shape of the curve reflects the rapid increase in temperature of the sample (with concomitant increase in the rate of peroxide decomposition) followed by a decrease in radical concentration which reflects the removal of the peroxide, and hence a reduction in the rate of alkoxy radical generation, *via* first-order decomposition at the elevated temperature reached. Calculations of the predicted radical concentrations (based on established data for the thermal decomposition of the peroxides) are discussed below. Tables 1, 2, and 3 which summarize

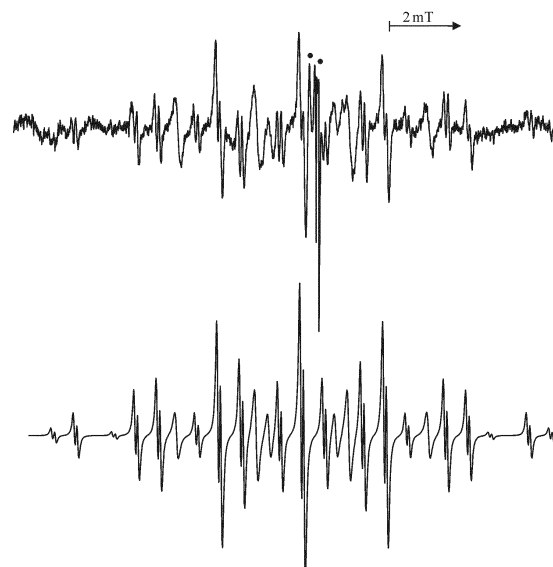


Fig. 1 EPR spectrum of radicals (14) and (15) obtained by photolysis of a mixture of 2,4-dimethylpentane (13) and di-*tert*-butyl peroxide at room temperature. The additional peaks (marked with ●) arise from the quartz sample cell. The lower trace shows the spectrum simulated using the parameters given in Table 2.

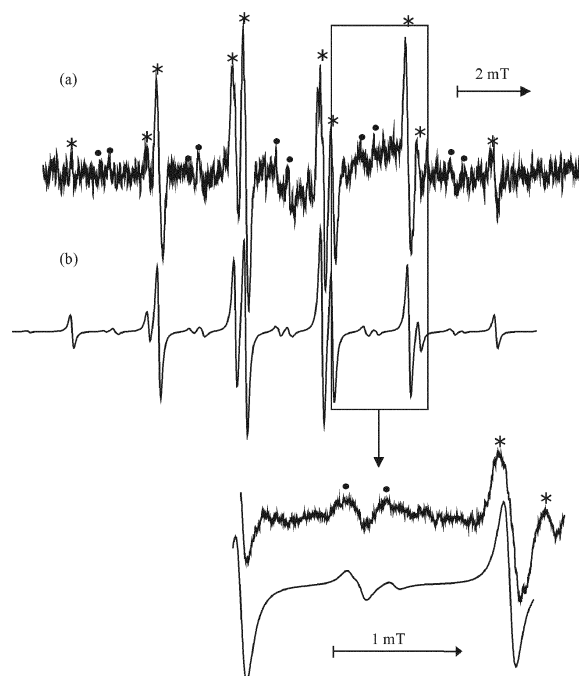
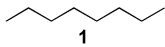
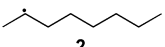
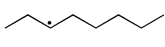
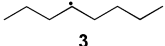
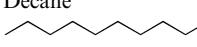
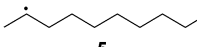
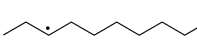
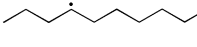
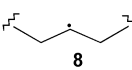
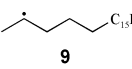
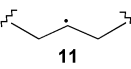


Fig. 2 EPR spectrum of radicals (8, *) and (9, ●) obtained by thermolysis of a mixture of eicosane (7) and 2,5-bis(*tert*-butylperoxy)-2,5-dimethylhexane at 443 K. The lower trace shows the spectrum simulated using the parameters given in Table 1.

results of EPR studies for linear alkanes, branched alkanes and linear alkenes, respectively, give the hyperfine splittings and relative radical concentrations as determined from spectrum simulation. Full details of procedures are provided in the experimental section.

(ii) **Linear alkanes: models for polyethylene (PE).** Reaction of both octane (1) and decane (4) under *photolytic* conditions with either peroxide at low temperature (263 K) and room temperature led to the detection of the EPR signals from the appropriate secondary radicals; there was no evidence of signals from primary radicals which could be formed by hydrogen-abstraction from the terminal methyl groups.¹ Two distinct signals were observed in each case (each with characteristic

Table 1 EPR parameters of radicals produced by hydrogen abstraction from linear alkanes by the *tert*-butoxyl radical

Substrate	Radical	Splitting constants/mT \pm 0.005			Ratio (%) \pm 5		
		α	β	γ	263 K ^a	298 K ^a	453 K ^b
		2.180	2.450 (CH ₃) 2.530 (CH ₂)	—	35	35	—
		2.185	2.530	0.080	65	65	—
							
Decane 		2.180	2.450 (CH ₃) 2.530 (CH ₂)	—	25	25	—
		2.185	2.530	0.080	75	75	—
							
C ₂₀ H ₄₂ Eicosane 7		2.185	2.480	—	—	—	90
		2.180	2.450 (CH ₃) 2.530 (CH ₂)	—	—	—	10
C ₄₀ H ₈₂ Tetracontane 10		2.185	2.480	—	—	—	100

^a Radicals generated by photolysis. ^b Radicals generated by thermolysis.

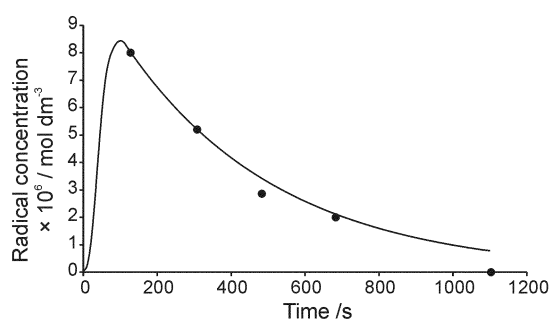


Fig. 3 Variation of the radical concentration *versus* time for radical (8) obtained by thermolysis of a mixture of eicosane and 2,5-bis(*tert*-butylperoxy)-2,5-dimethylhexane at 443 K. The solid line shows the predicted radical concentration modelled allowing for variation of the rate of decomposition of the peroxide with temperature and using a radical–radical termination rate of $2 \times 10^8 \text{ dm}^3 \text{ mol}^{-1} \text{ s}^{-1}$.

alkyl radical *g*-values of 2.0026 ± 0.0001). The first is associated with a radical with typical β -methyl and methylene groups (quartet and triplet, respectively), *i.e.* (2) for octane and (5) for decane. The second shows a β -quintet which is associated with the “mid-chain” structure $-\text{CH}_2\dot{\text{C}}\text{HCH}_2-$, *i.e.* (3) for octane and (6) for decane. The characteristic hyperfine splittings and assignments are given in Table 1: the values of a_{Me} for the methyl attached to the radical centre are entirely as expected¹³ and the β -methylene splitting for (3) and (6) leads to a calculated¹⁴ average value of θ of *ca.* 45° *i.e.* there is relatively free rotation about the $\text{C}_\alpha-\text{C}_{\beta\text{-methylene}}$ bond.

Relative concentrations of the two species in each case (determined by spectral simulation) were found to be, within experimental error, as predicted from statistical attack on the substrate (*i.e.* equal rate of attack at each of the methylene groups, see Table 1) on the assumption that small alkyl radicals have the same termination rate.¹⁵ The upper limit for the relative concentration of (undetected) primary radicals is 5%.

For eicosane, (C₂₀H₄₂) (7), EPR spectra obtained under thermolytic conditions (see, *eg.*, Fig. 2) were dominated by signals from mid-chain radical(s) (8) with splittings similar to the analogous radicals observed in the photolysis experiments

with octane or decane. Weak signals were observed due to H-abstraction from the methylene group nearest the end of the chain(9), again characterised by β -methyl and β -methylene splittings. Again, the selectivity of attack on the different methylene groups appears to be statistical. Similarly, tetracontane (C₄₀H₈₂) (10) gave signals from mid-chain radicals; however, in this case abstraction from the terminal methylene group (*i.e.* C2 and C19) was not observed. The upper limit for the concentration of radicals arising from H-abstraction from the end-most methylene group is $\sim 5\%$, the limit of detection in these experiments. The calculated profile for the variation of radical concentration as a function of time for (8) (Fig. 3) takes into account the variation of sample temperature at the start of the reaction (and hence changes in the rate constant for peroxide homolysis¹⁶) as well as the decrease in peroxide concentration with time. A good fit to the experimental data was obtained using a rate constant for termination ($2k_t$) of *ca.* $2 \times 10^8 \text{ dm}^3 \text{ mol}^{-1} \text{ s}^{-1}$. This value presumably reflects the viscosity of the medium (*cf.* values of *ca.* $10^9 \text{ dm}^3 \text{ mol}^{-1} \text{ s}^{-1}$ for small radicals in non-viscous solution).

In both photolysis and thermolysis experiments with 2,5-bis(*tert*-butylperoxy)-2,5-dimethylhexane (Trigonox 101) the signals from radicals derived from the alkane were accompanied by a further signal with splittings $a_{2\text{H}} 2.20$, $a_{1\text{H}} 2.49$, $a_{1\text{H}} 2.43$ mT and *g*-value 2.0026 typical of the primary radical structure $\dot{\text{C}}\text{H}_2\text{CH}_2-$; this was not observed when using di-*tert*-butyl peroxide. This signal is attributed to the radical (12) which arises from β -scission of the alkoxy radical, itself formed on peroxide homolysis (see Scheme 1). Photolytic decomposition of 2,5-bis(*tert*-butylperoxy)-2,5-dimethylhexane dissolved in benzene (*i.e.* in the absence of a suitable substrate) gave an identical EPR signal.

In summary, for the linear alkanes secondary radicals originate from H-abstraction from methylene groups, in a ratio corresponding to the statistical distribution of the methylene groups ($\text{CH}_3\text{CH}_2-\text{R}$ and $\text{R}-\text{CH}_2\text{CH}_2\text{CH}_2-\text{R}$, see Table 1). The absence of primary radicals evidently reflects a lower rate of abstraction from the terminal methyl groups, although their disappearance by rapid inter- or intramolecular hydrogen-abstraction cannot be ruled out at this stage.

Table 2 EPR parameters of radicals produced by hydrogen abstraction from branched alkanes by the *tert*-butoxyl radical

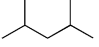
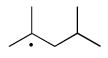
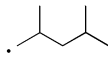
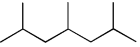
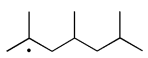
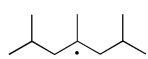
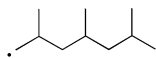
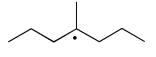
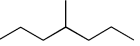
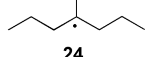
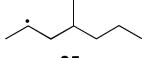
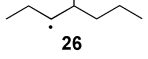
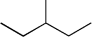
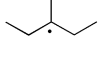
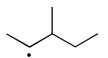
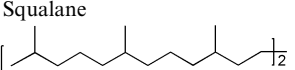
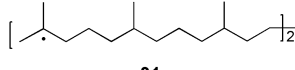
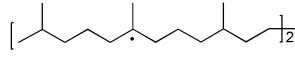
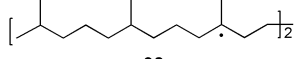
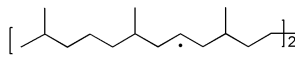
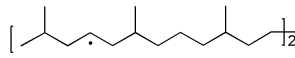
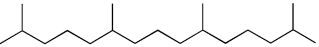
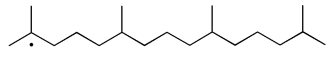
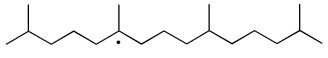
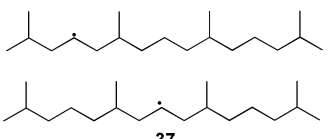
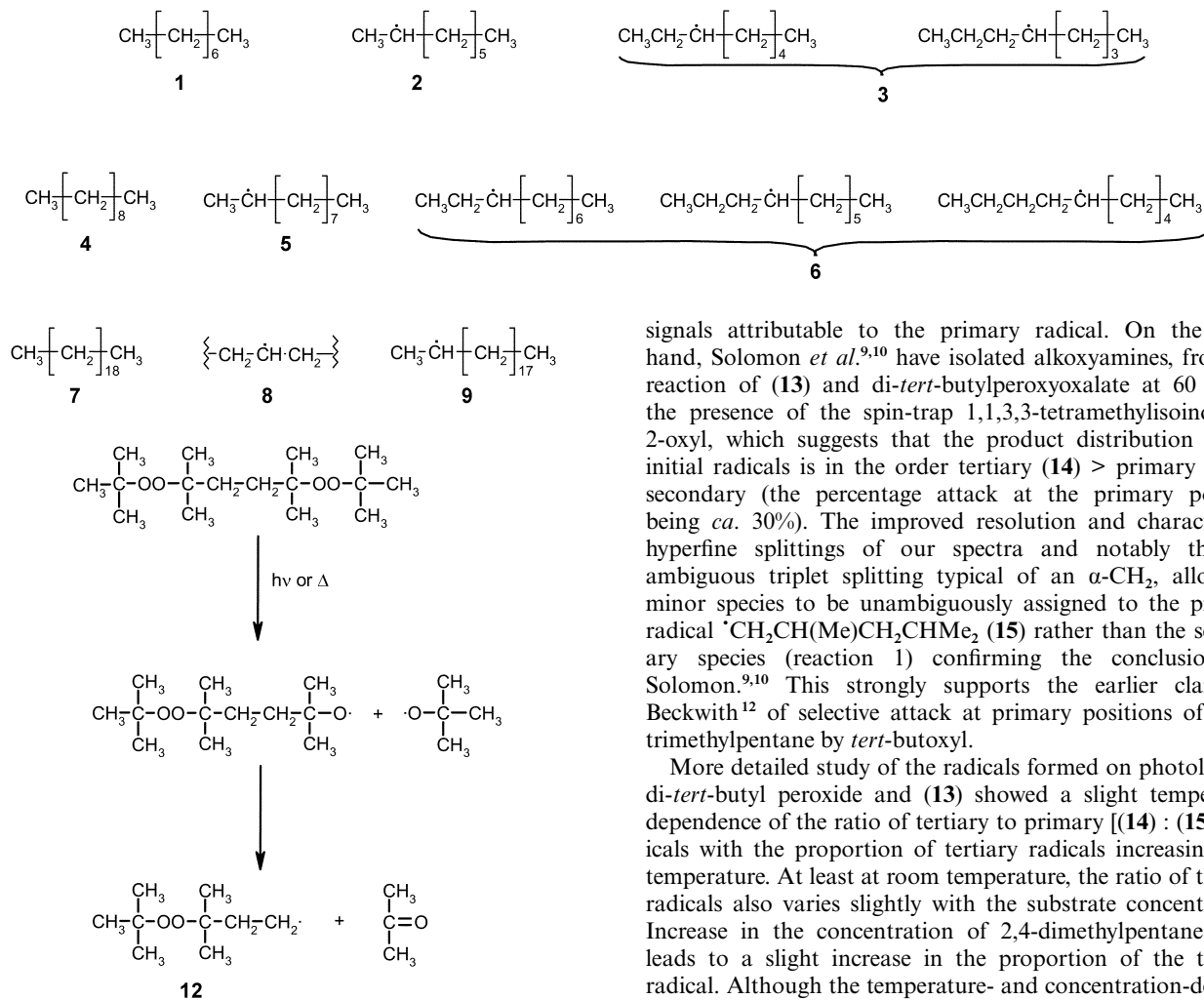
Substrate	Radical	Splitting constants/mT \pm 0.005			Ratio (%) \pm 5		
		α	β	γ	263 K ^a	298 K ^a	453 K ^b
2,4-Dimethylpentane  13	 14	—	2.340 (CH ₃) 1.710 (CH ₂)	0.100	65	75	—
	 15	2.245	2.610	—	35	25	—
2,4,6-Trimethylheptane  19	 20	—	2.300 (CH ₃) 1.545 (CH _{2x}) 1.865 (CH _{2y})	0.100	43	57	—
	 21	—	2.530 (CH ₃) 1.620 (CH ₂)	—	32	43	—
	 22	2.185	2.630	—	25	0	—
	 23	—	2.300 (CH ₃) 1.800 (CH ₂)	0.100	—	60	—
4-Methylheptane  23	 24	—	2.300 (CH ₃) 1.800 (CH ₂)	0.100	—	60	—
	 25	2.185	2.430 (CH ₃) 2.560 (CH ₂)	—	—	30	—
	 26	2.200	2.200 (CH ₂) 1.770 (CH)	—	—	10	—
3-Methylpentane  27	 28	—	2.350 (CH ₃) 1.850 (CH ₂)	—	—	50	—
	 29	2.190	2.530 (CH ₃) 1.920 (CH)	—	—	50	—
Squalane  30	 31	—	2.300 (CH ₃) 1.825 (CH _{2x}) 1.755 (CH _{2y})	0.090	40 ^c	—	30
	 32	—	2.265 (CH ₃) 1.825 (CH ₂)	0.080	60 ^c	—	35
	 33	2.165	2.380 (CH _{2x}) 2.300 (CH _{2y})	—	—	—	35
	 34	—	2.301 (CH ₃) 1.825 (CH _{2x}) 1.755 (CH _{2y})	0.090	50 ^c	—	33
	 35	—	2.265 (CH ₃) 1.825 (CH ₂)	0.080	50 ^c	—	33
2,6,10,14-Tetramethylpentadecane  34	 35	—	2.301 (CH ₃) 1.825 (CH _{2x}) 1.755 (CH _{2y})	0.090	50 ^c	—	33
	 36	—	2.265 (CH ₃) 1.825 (CH ₂)	0.080	50 ^c	—	33

Table 2 (Contd.)

Substrate	Radical	Splitting constants/mT \pm 0.005			Ratio (%) \pm 5		
		α	β	γ	263 K ^a	298 K ^a	453 K ^b
	 37	2.165	2.380 (CH _{2x}) 2.300 (CH _{2y})	—	—	—	33

^a Radicals generated by photolysis. ^b Radicals generated by thermolysis. ^c at 233 K.



Scheme 1

(iii) **Branched-chain alkanes: models for polypropylene (PP) and polyethylene-propylene copolymers (EPM).** 2,4-Dimethylpentane (**13**) photolysis of di-*tert*-butyl peroxide with 2,4-dimethylpentane (**13**) gave EPR spectra from a mixture of two radicals with hyperfine splittings a_{6H} 2.340, a_{2H} 1.710, a_{1H} 0.100 mT and a_{2H} 2.245, a_{1H} 2.610 mT, respectively (see Table 2) and g -value 2.0026. The former is assigned to the tertiary radical \cdot CMe₂CH₂CHMe₂ (**14**), with characteristic β -proton splittings, similar to those (less well-resolved) signals obtained in CIDEP studies of the photolysis of propanone in this solvent.¹¹ The remaining signals may be assigned either to the *secondary* radical \cdot CH(CHMe₂)₂ or to the *primary* radical \cdot CH₂CH(Me)CH₂CHMe₂ (**15**), hence further detailed consideration is necessary. Thus, in CIDEP studies,¹¹ an additional radical (weak signals) with splittings 2.27 (2H) and 2.30 (1H) mT was assigned to the *secondary* radical \cdot CH(CHMe₂)₂, with no

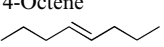
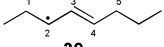
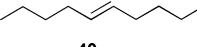
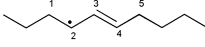
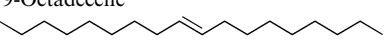
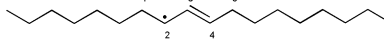
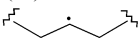
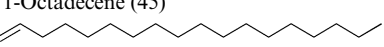
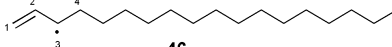
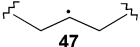
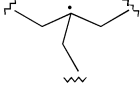
signals attributable to the primary radical. On the other hand, Solomon *et al.*^{9,10} have isolated alkoxyamines, from the reaction of (**13**) and di-*tert*-butylperoxyoxalate at 60 °C, in the presence of the spin-trap 1,1,3,3-tetramethylisindoline-2-oxyl, which suggests that the product distribution of the initial radicals is in the order tertiary (**14**) > primary (**15**) > secondary (the percentage attack at the primary position being *ca.* 30%). The improved resolution and characteristic hyperfine splittings of our spectra and notably the unambiguous triplet splitting typical of an α -CH₂, allow the minor species to be unambiguously assigned to the primary radical \cdot CH₂CH(Me)CH₂CHMe₂ (**15**) rather than the secondary species (reaction 1) confirming the conclusions of Solomon.^{9,10} This strongly supports the earlier claim by Beckwith¹² of selective attack at primary positions of 2,2,4-trimethylpentane by *tert*-butoxyl.

More detailed study of the radicals formed on photolysis of di-*tert*-butyl peroxide and (**13**) showed a slight temperature dependence of the ratio of tertiary to primary [(**14**) : (**15**)] radicals with the proportion of tertiary radicals increasing with temperature. At least at room temperature, the ratio of the two radicals also varies slightly with the substrate concentration. Increase in the concentration of 2,4-dimethylpentane again leads to a slight increase in the proportion of the tertiary radical. Although the temperature- and concentration-dependence would be consistent with an intermolecular reaction (2) of primary radicals (**15**) with 2,4-dimethylpentane to give the tertiary radical (**14**), no further conclusive evidence could be obtained in experiments described overleaf.

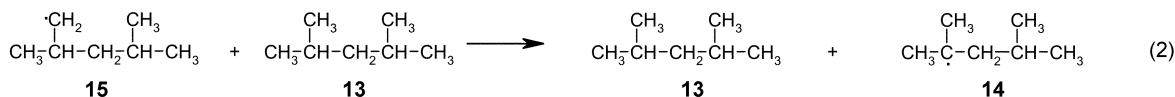
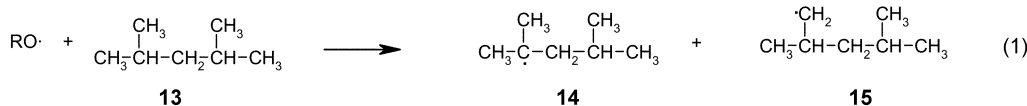
The increase in the concentration of (**14**) could, in principle, also arise from attack at this C–H by methyl radicals (derived by an increased rate of fragmentation of *tert*-butoxyl as the temperature is raised). However, calculations involving activation energies⁶ and rates of *tert*-butoxyl attack¹⁷ and fragmentation¹⁷ show that this reaction is not likely to be significant at room temperature. The low boiling point of 2,4-dimethylpentane precluded study under thermolytic conditions.

Related spin-trapping experiments involving the photolysis of di-*tert*-butyl peroxide and 2,4-dimethylpentane (2 : 1 v/v) in the presence of 2,4,6-tri-*tert*-butylnitrosobenzene (12 mM) at room temperature gave EPR spectra which contained signals from two radical adducts. The dominant signal is an *anilino* species (formed by radical addition to the nitroso oxygen),¹⁸

Table 3 EPR parameters of radicals produced by hydrogen abstraction from linear alkenes by the *tert*-butoxyl radical

Substrate	Radical	Splitting constants/mT \pm 0.005			Ratio (%) \pm 2.5		
		α	β	γ	263 K ^a	298 K ^a	443 K ^b
4-Octene 	 39	1.420 (H ₂) 1.445 (H ₄) 0.375 (H ₃)	1.365 (H _{1,s})	—	100	100	—
5-Decene 	 41	1.350 (H _{2,4}) 0.430 (H ₃) 1.270 (H _{2,4}) 0.350 (H ₃)	1.350 (H _{1,s}) 1.270 (H _{1,s})	—	77 23	77 23	—
9-Octadecene 	 43	1.350 (H _{2,4}) 0.430 (H ₃) 1.270 (H _{2,4}) 0.350 (H ₃)	1.350 (H _{1,s}) 1.270 (H _{1,s})	—	60 30	60 30	65 35
	(44)  44	2.120	2.500	—	10	10	—
1-Octadecene (45) 	 46	1.470 (H _{1,exo}) 1.360 (H _{1,endo}) 0.370 (H ₂) 1.320 (H _{3,endo})	1.280 (H ₄)	—	50	50	40
	 47	2.120	2.500	—	50	50	40
	 48	—	1.880	—	—	—	20

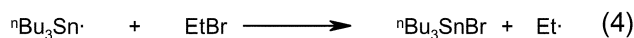
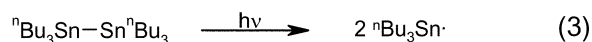
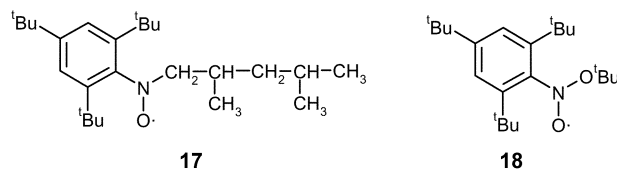
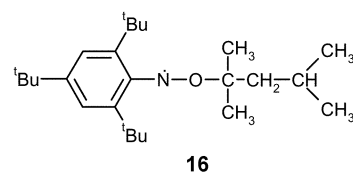
^a Radicals generated by photolysis. ^b Radicals generated by thermolysis.



with a_{N} 0.965 and $a_{\text{meta-2H}}$ 0.205 mT, g 2.0041, characteristic of the trapping of a tertiary radical (**16**) and assigned as an adduct of (**14**), see Table 2. The other signals are assigned to a *nitroxide* (with a_{N} 1.34, $a_{\beta\text{-1H}}$ 1.73, $a_{\beta\text{-1H}}$ 1.85 mT, g 2.0060) characteristic of the trapping of a *primary* radical. This is assigned to (**17**), arising from trapping of the primary radical (**15**), in which the inequivalence of the β -protons of this nitroxide is attributed to the presence of the chiral centre at the γ -position; for a discussion of the underlying principles and some related examples see, *e.g.*, ref. 19). No signals from the trapping of a secondary species were detected. At high trap concentration (50 mM), only signals with a_{N} 2.35 mT, g 2.0060 could be observed. These are typical of an alkoxy nitroxide and assigned to the *tert*-butoxyl adduct (**18**).

The spin-trapping results are thus also consistent with initial hydrogen abstraction by *tert*-butoxyl from 2,4-dimethylpentane occurring predominantly from the tertiary positions with minor attack at primary sites, in general agreement with direct EPR observations and product studies.⁹

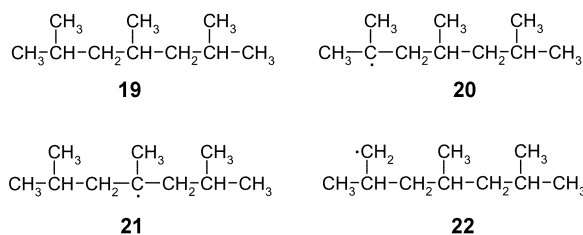
In order to test the possibility of intermolecular hydrogen-abstraction from tertiary hydrocarbons by primary radicals, ethyl radicals were produced by photolysis of hexa-*n*-butylditin in the presence of bromoethane (1 : 1 v/v, reactions 3 and 4) and detected by EPR. Inclusion of 2,4-dimethylpentane in the mixture (1 : 1 : 1) in experiments at room temperature did not affect the EPR spectrum. Therefore, there is no significant



intermolecular reaction of primary radicals with 2,4-dimethylpentane under the conditions employed.

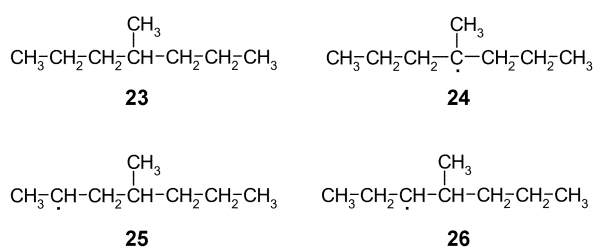
2,4,6-Trimethylheptane. The EPR spectra obtained from 2,4,6-trimethylheptane (**19**) under photolytic steady-state conditions at 263 K similarly allowed the two tertiary radicals (**20**)

and (21) to be identified unambiguously. Of particular note for the former are the non-equivalent β -proton splittings ($a_{\beta\text{-IH}}$ 1.545, $a_{\beta\text{-IH}}$ 1.865 mT), observed under all conditions employed, a phenomenon which reflects the chirality of the γ -carbon. An additional radical with $a_{2\text{H}}$ 2.185, a_{H} 2.630 mT, present at a relative concentration of *ca.* 25%, is assigned to the primary radical (22) as its splittings are virtually identical to those of radical (15) observed for 2,4-dimethylpentane. Variation of the concentration of 2,4,6-trimethylheptane (19) did not affect the ratio of primary to tertiary radicals observed. When experiments were carried out at room temperature, only signals from the two tertiary radicals (20) and (21) were detected. Our results appear to rule out intermolecular H-abstraction by (22) from 2,4,6-trimethylheptane (19) to generate (20) or (21): intramolecular hydrogen-abstraction (1,4, or 1,6) would not be expected to be important.



Spin-trapping studies involving photolysis of a mixture of di-*tert*-butyl peroxide and 2,4,6-trimethylheptane in the presence of 2,4,6-tri-*tert*-butylnitrosobenzene (1.25 mM) at room temperature gave strong signals from an anilino radical adduct (with a_{N} 0.965, $a_{\text{meta-2H}}$ 0.205 mT, g 2.0041) which arises from the trapping of tertiary alkyl radicals, presumably (20) and (21). At higher trap concentrations (50 mM), additional signals were observed from a nitroxide (with a_{N} 1.34, $a_{\beta\text{-IH}}$ 1.73, $a_{\beta\text{-IH}}$ 1.85 mT, g 2.0060) characteristic of the trapping of the primary radical (22), as well as the *tert*-butoxyl adduct (18).

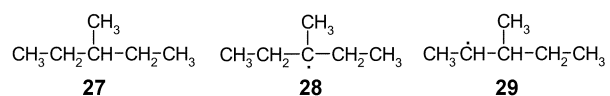
4-Methylheptane. For both 2,4-dimethylpentane (13) and 2,4,6-trimethylheptane (19), we conclude that the methylene-group protons are particularly unreactive. In contrast, the EPR spectrum obtained from 4-methylheptane consists of signals from at least three radicals: signals from the tertiary radical (24) are dominant (~60%), together with the two secondary radicals (25) and (26) (*ca.* 30% and 10% respectively), indicating a relatively high reactivity of the CH₂ hydrogens in this molecule.



For the branched alkanes (13) and (19), literature suggests^{9,10} steric crowding from the methyl groups reduces the rate of hydrogen-abstraction at the tertiary position, and for the methylene groups, the reduction in rate is such that abstraction is not observed from this position (see also refs. 9, 10 and 12). A

significant amount of initial hydrogen abstraction by *tert*-butoxyl occurs from the methyl groups to give primary radicals (not observed for linear alkanes).

3-Methylpentane. The EPR spectrum obtained from 3-methylpentane (27) consists of signals from the tertiary radical (28) and the secondary radicals (29) in equal concentration. This is again consistent with a relatively high reactivity of the CH₂ hydrogens towards abstraction by *tert*-butoxyl. Independent generation of ethyl radicals in the presence of 3-methylpentane, see above, showed no evidence for intermolecular hydrogen-abstraction from the secondary or tertiary sites, at room temperature.



Squalane. The triterpene squalane (30), a model for alternating ethylene-propylene copolymers, allowed EPR studies to be carried out under both photolytic (low temperatures) and thermolytic (high temperature) conditions, the latter comparable to those under which polymers have been studied.²⁰ The EPR spectrum obtained during photolysis of a mixture of di-*tert*-butyl peroxide and squalane (1 : 2 v/v) at 233K contained signals from two types of tertiary alkyl radical, (31) and (32): arrows on (30) indicate site of attack for generation of radicals (31), (32) and (33). The former is characterised by the splittings from two β -methyl groups ($a_{\beta\text{H}}$ 2.300 mT), a β -methylene group ($a_{\beta\text{H}}$ 1.825, $a_{\beta\text{H}}$ 1.755 mT) and a small triplet splitting from the γ -CH₂ group ($a_{2\text{H}}$ 0.09 mT); the β -CH₂ protons are inequivalent due to the presence of the ϵ chiral-centre. However, the relatively large distance between the chiral centre and the β -CH₂ makes the inequivalence small (0.07 mT) compared to that observed for (20) (0.32 mT) which contains a γ chiral-centre. The remaining signals arise from the two mid-chain tertiary radicals [(32)]. Their greater line-width compared to that of (31) is presumably due to slight differences in the splittings for each species and also small differences in the β -CH₂ splittings within each species (although a quintet from the 4 γ -protons is still observable). The larger line-width is also likely to mask any inequivalence in the β -CH₂ splittings arising from the ϵ -chiral centre. When experiments were carried out at 453 K with thermal decomposition of the peroxide (2 : 1 v/v), additional signals were observed from secondary radicals (33); reduction in selectivity is believed to reflect the significantly higher temperature.

2,6,10,14-Tetramethylpentadecane (Pristane). Pristane (34), like squalane, gave signals solely from two tertiary radicals (35) and (36) in equal concentrations, with splittings, as expected, closely similar to the equivalent radicals derived from squalane [(31) and (32), respectively]; arrows on (34) indicate site of attack for generation of radicals (35), (36) and (37). These results are consistent with the rates of hydrogen-abstraction being the same for each of the methine groups. At high temperature, additional signals were observed from secondary radicals (37) (as for squalane).

(iv) Linear alkenes. In order to determine the relative selectivity of hydrogen-abstraction from alkyl C-H versus allyl C-H bonds, the reaction of peroxide-derived radicals with a range of linear alkenes (see Table 3) was studied. Previous EPR studies⁴

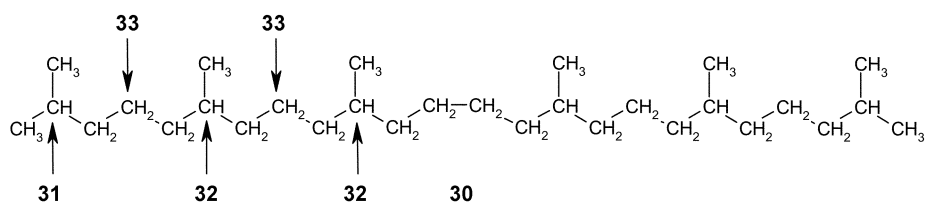
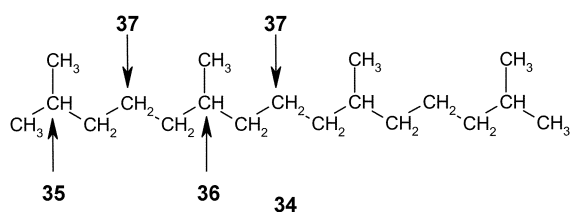


Table 4 Rate constants for hydrogen abstraction from alkanes and alkenes by *tert*-butoxyl at 293 K^a

Molecule	Group	Overall rate constant/ 10 ⁴ dm ³ mol ⁻¹ s ⁻¹	Rate constant (per CH)/ 10 ⁴ dm ³ mol ⁻¹ s ⁻¹
Decane	CH ₂	71	4.4
2,4-Dimethylpentane	CH	17	6.5
	CH ₃		0.3
	CH		13.8
3-Methylheptane	CH ₂	28	3.5
	CH		16.6
4-Methylheptane	CH	29	2.1 ^b
	CH ₂		0.9 ^c
	CH ₂		36
4-Octene	CH ₂ allyl	144	36
5-Decene	CH ₂ allyl	144	36
9-Octadecene	CH ₂ allyl	148	37

^a ± 30% ^b .Rate for 2 and 6 positions. ^c Rate for 3 and 5 positions.



of the thermolytic decomposition of peroxides incorporated in polyethylene revealed allyl radicals, in addition to the expected secondary alkyl radicals formed by hydrogen-abstraction from the polymer chain, with the relative concentration of the former increasing with time.

Photolysis of di-*tert*-butyl peroxide with 4-octene (**38**) and 5-decene (**40**) at room temperature and 263 K gave EPR spectra solely from the respective allyl radicals formed by hydrogen-abstraction adjacent to the double bond (see Table 3). For 9-octadecene, two isomeric alkyl radicals (**43**) were observed. As reported previously,²¹ the major species is assigned to the allyl radical with both alkyl chains *exo* and the minor to the isomer with one *exo* and one *endo* alkyl chain and additional signals were observed from secondary alkyl radicals (**44**). From the relative concentrations of the allyl and alkyl radicals we estimate that the rate constant for attack at an allylic CH₂ group is approximately 45 times faster than abstraction from the other methylene groups. The EPR spectrum from 1-octadecene (**45**) again gave signals from the corresponding allyl radical (**46**). As with 9-octadecene, there were also signals present from secondary alkyl radicals (**47**) formed by hydrogen-abstraction from the non-allylic CH₂ groups. The ratio of the rates of attack of allylic-CH₂ versus alkyl-CH₂ is *ca.* 13 : 1 for this molecule.

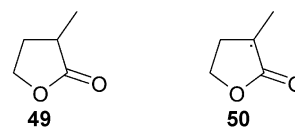
Photolytic generation of ethyl radicals (*via* reactions 3 and 4) in the presence of 5-decene (1.75 mol dm⁻³) at room temperature gave an EPR spectrum containing signals from both the ethyl radical and the allyl radical (**41**) derived from 5-decene, in a ratio of 1 : 1.25, respectively. This observation is consistent with a relatively rapid intermolecular hydrogen-abstraction from the allylic position of 5-decene by the primary ethyl radicals. Using steady-state kinetic analysis, we estimate that the rate of hydrogen abstraction by ethyl from decene is 1.4 × 10³ dm³ mol⁻¹ s⁻¹. Use of 2-bromopropane instead of bromoethane gave an EPR spectrum with signals solely from 2-propyl radicals; No signals from allyl radicals were observed. Evidently, whilst the rate of hydrogen abstraction from 5-decene by primary radicals is fast at room temperature, the equivalent hydrogen abstraction by secondary radicals is too slow to be observed by EPR under these conditions.

(b) Determination of rates of hydrogen abstraction

At this stage, we can conclude that, as expected for linear and many of the branched alkanes, the order of reactivity of

unhindered C–H bonds is as follows: CH_{2(allylic)} > CH > CH₂ > CH₃ with a relative reactivity per hydrogen (*e.g.* at 298 K) of 8.2 (allylic) : 3.1 (tertiary) : 1 (secondary) : >> 1 (primary). These results are broadly comparable to those of Walling and Jacknow⁷ (CH vs CH₂ 3.6 : 1) and to those we have calculated from the review of appropriate kinetic parameters given by Howard *et al.*⁶ Use of these parameters (*E_a*, *A*) leads to a prediction of 8 : 3.3 : 1 : 0.067 at 298 K. In contrast, for the hindered molecules 2,4-dimethylpentane, and 2,4,6-trimethylheptane, we conclude that the ratio is in the order: CH > CH₃ > CH₂.

In order to obtain more detailed information, we have estimated absolute rate constants by performing a series of competition reactions with α -methyl- γ -butyrolactone as standard as its rate constant for reaction with *tert*-butoxyl is known (5 × 10⁵ dm³ mol⁻¹ s⁻¹ at room temperature).² Photolysis of a mixture α -methyl- γ -butyrolactone (**49**), decane (**4**) and di-*tert*-butyl peroxide (1 : 10 : 11 v/v) at room temperature (293 K) gave an EPR spectrum consisting of signals from the decane-derived radicals (**5**) and (**6**) and the lactone-derived radical (**50**). The rate constants for hydrogen-atom abstraction from the CH₂ groups of decane can be determined from the relative concentrations of radicals (**5**), (**6**) and (**50**), assuming that the rate constant for radical–radical termination of the three species is the same. For decane, we obtain a rate constant of 4.4 × 10⁴ dm³ mol⁻¹ s⁻¹ (per hydrogen) for abstraction of hydrogens from the CH₂ groups at 293 K.



This approach was then extended to mixtures of the lactone (**49**), a hydrocarbon (linear or branched alkane or linear alkene) and di-*tert*-butyl peroxide. The hydrocarbons were chosen to allow the rate constants for hydrogen abstraction by *tert*-butoxyl from CH₃, CH₂, CH (both hindered and unhindered) and allylic-CH₂ to be determined. The results, which are collected together in Table 4, give rate constants in the range 3 × 10³ – 3.7 × 10⁵ dm³ mol⁻¹ s⁻¹ which may be compared with typical values obtained for hydrogen abstraction from other substrates including ethers (2 × 10⁶ to 8 × 10⁶ dm³ mol⁻¹ s⁻¹),^{22,23} ketones (1 × 10⁶ to 2 × 10⁶ dm³ mol⁻¹ s⁻¹),² esters (2 × 10⁴ to 5 × 10⁵ dm³ mol⁻¹ s⁻¹)² and cycloalkanes (C₅H₁₀ 1 × 10⁶ dm³ mol⁻¹ s⁻¹, C₆H₁₂ 9 × 10⁵ dm³ mol⁻¹ s⁻¹).¹⁷

Further experiments were carried out on mixtures containing two hydrocarbons and di-*tert*-butyl peroxide, the pairs of the former chosen to allow the individual radicals from each species to be discriminated. From the ratios of the radicals observed (taking into account the concentrations of the hydrocarbons in the mixture), the relative rates of attack were determined. For

mixtures of two alkanes, the relative rates of attack matched those expected from the rate constants determined from the competition experiments of alkanes with α -methyl- γ -butyrolactone (49). Mixtures containing an alkane and an alkene, however, gave higher proportions of allylic radicals than expected from the rate constants determined above and given in Table 4. We believe that this is due to the reaction of the alkyl radicals (from hydrogen-abstraction by *tert*-butoxyl from the alkane) with the alkene to give additional allyl radicals.

(c) DFT quantum calculations on hydrogen-atom abstraction

The most notable experimental finding is that for reaction of 2,4-dimethylpentane or 2,4,6-trimethylheptane with *tert*-butoxyl radicals, tertiary radicals (major) and primary radicals (minor) but no secondary radicals are observed. That tertiary C–H bonds are the most labile of the three kinds, and therefore give rise to higher concentrations of tertiary radicals when the branched alkane reacts with a *tert*-butoxyl radical, is expected from the behaviour of linear alkanes (where abstraction from CH₂ rather than CH₃ is observed). However, the absence of secondary radicals seems unexpected. Several authors have suggested^{7–12} that this is due to steric reasons without further in-depth or numerical analysis supporting such a statement. From inspection of a 3D molecular model, however, there does not seem to be any *a priori* reasons of steric congestion why the secondary radical should not be formed. Further, if this were true, the tertiary radical would be expected to form with even greater difficulty.

Fokin and Schreiner in a recent review paper on selective alkane transformations *via* radicals and radical cations²⁴ described only a modest correlation between C–H BDE's (bond dissociation energies) and alkane activation. They note that the activation mechanisms are less simple than they may appear at first sight. Similar consideration may apply for the compounds and processes described here. Thus, we calculated the BDE's for all of the systems studied in this paper and a consistent set of values was obtained in the expected order tertiary (418 kJ mol⁻¹) < secondary (435 kJ mol⁻¹) < primary (452 kJ mol⁻¹). Thus, the BDE's clearly do not explain the order as observed for, *e.g.*, 2,4-dimethylpentane.

Next, the full potential energy profiles for hydrogen-abstraction from each different type of hydrogen in 2,4-dimethylpentane were calculated. These are shown in Fig. 4, and reveal that the barriers for tertiary secondary and primary radical formation are 42, 48 and 51 kJ mol⁻¹, respectively, again as predicted from a simple thermodynamic approach. These values imply that rate is fastest for tertiary radical formation, followed by secondary and then primary. The 9 kJ mol⁻¹ difference between tertiary and primary implies approximately an order of magnitude difference in kinetics. That the differences are not simply a result of steric hindrance is shown by the space-filling models of the three transition state structures, revealing essentially no atom–atom overlap (see ESI †). However to obtain more reliable rates, we should compare the free energy differences for the van der Waals like state ($r(\text{O–H}) = 2.5 \text{ \AA}$) and the transition state, in each case. We find that the effect [*i.e.* the difference between $(\text{H} - \text{TS})_{\text{trans.state}}$ and $(\text{H} - \text{TS})_{\text{vdW}}$] for tertiary radical formation is non-negligible (-5.4 kJ mol^{-1}), for secondary radical formation is small (-2.1 kJ mol^{-1}) but for primary radical formation is *not small* ($-10.0 \text{ kJ mol}^{-1}$). This last number implies that the 9 kJ mol⁻¹ energy difference between tertiary and primary radical formation as noted above (*i.e.* just ΔE) is reduced by about 4.2 kJ mol⁻¹. This result, which presumably reflects varying entropy contributions in the transition states, *qualitatively* explains the experimental observation for 2,4-dimethylpentane of roughly equal amounts of tertiary and primary radicals (with more tertiary than primary) and the lower concentration of secondary radicals, undetectable by EPR.

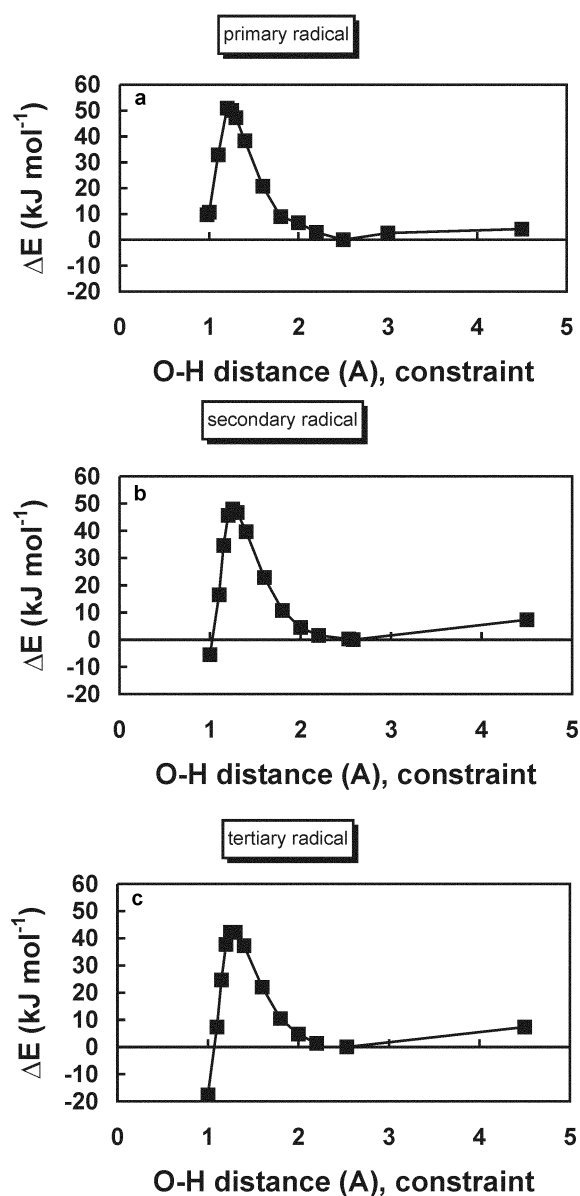


Fig. 4 Calculated energy profile (DFT level of theory) for hydrogen-abstraction by *tert*-butoxyl from the primary, secondary and tertiary positions of 2,4-dimethylpentane.

3 Conclusions

We report a consistent set of EPR data on a series of low molecular weight alkanes, both linear and branched, and some alkenes, representing the characteristic moieties in polyethylenes, polypropylenes and EPM rubbers. The results are interpreted in terms of relative C–H abstraction rates by *tert*-butoxyl radical attack in a consistent and satisfactory way. In accordance with relative bond dissociation energies, allylic radicals are formed most easily from alkenes. Similarly, in linear alkanes the order of abstraction follows the BDE's: primary radicals are far more difficult to form than secondary using the peroxides employed here. For branched systems, however, the presence of primary radicals and the absence of detectable amounts of secondary radicals cannot be explained simply in terms of differences in BDE's. Quantum mechanical modelling of the activation free energies, which govern the kinetics of the reactions, have revealed that the entropy term is responsible for the higher rate of abstraction from primary C–H bonds for the highly branched, *i.e.* $-\text{CH}_2-\text{CH}(\text{Me})-\text{CH}_2-\text{CH}(\text{Me})-$ sequences. This consistent set of results forms the starting point for the interpretation of polymer EPR spectra to be discussed in a subsequent paper.

4 Experimental

All chemicals were commercially available samples and used without further purification. Compounds obtained from Aldrich included di-*tert*-butyl peroxide, 2,5-bis(*tert*-butylperoxy)-2,5-dimethylhexane (Luperox-101, Trigonox-101), hexabutyliditin, 3-methylpentane, 4-methylheptane, 4-octene, 5-decene, 1-octadecene, 2,4-dimethylpentane, squalane, 2,6,10,14-tetramethylpentadecane, α -methyl- γ -butyrolactone, bromoethane, 2-bromopropane and 2,4,6-tri-*tert*-butylnitrosobenzene. Lancaster Synthesis supplied octane, decane, eicosane and tetracontane. We obtained 2,4,6-trimethylheptane from Chem-sampco and 9-octadecene from Avocado.

EPR spectra were recorded on a Bruker ESP300 EPR spectrometer equipped with an X-band microwave bridge. Temperature control was achieved using a Bruker ER-4111 variable-temperature controller, the temperature at the centre of the EPR cavity was calibrated using an separate thermocouple. *In-situ* photolysis was carried out using the unfiltered radiation of a Hanovia 977B-1 1 kW mercury-xenon arc lamp focused onto the cell through the front grill of the cavity.

For photolysis experiments, the alkane or alkene substrate was mixed with the peroxide (typically 1 : 1 v/v) and placed in a quartz sample tube (od 4.0 mm). The tube was placed in the cavity of the EPR spectrometer and the EPR spectrum recorded whilst irradiating the sample with UV light. The spectrum was normally acquired over 20 minutes. Typical spectrometer parameters were: centre field 333.3 mT; sweep width 15 mT; scan time 1342.18 s; time constant 1310.72 ms; modulation frequency 9.35 GHz; modulation amplitude 0.10 mT; microwave power 2 mW.

For thermolysis experiments, the alkane or alkene substrate was mixed with the peroxide (typically 1 : 1 v/v) and placed in a borosilicate sample tube (od 5.0 mm). The EPR cavity was preheated to the required temperature (typically 453 K) and once achieved, the sample was placed in the cavity of the spectrometer. The sample subsequently reached the required temperature within 50 seconds. A number of spectra were then recorded until EPR signals could no longer be observed (after about 15 min). Each spectrum usually took 160 seconds to acquire. The half-lives of the peroxides have been estimated from their reported activation parameters.¹⁶ For 2,5-bis(*tert*-butylperoxy)-2,5-dimethylhexane the half-lives are estimated to be 85 s at 443 K and 35 s at 453 K. Similarly, for di-*tert*-butyl peroxide the half-lives are estimated to be 205 s at 443 K and 80 s at 453 K. Typical spectrometer parameters were: centre field 333.3 mT; sweep width 15 mT; scan time 10.49 s; time constant 10.24 ms; modulation frequency 9.35 GHz; modulation amplitude 0.16 mT; microwave power 10 mW.

Absolute radical concentrations were determined by comparison of the double integrals of the experimental spectra with that of a standard weak pitch sample under identical spectrometer conditions. The pitch sample was calibrated by comparison (at room temperature) with the spectrum obtained from a solution of the stable nitroxide 4-hydroxy-2,2,6,6-tetramethylpiperidine-1-oxyl (TEMPOL) at known concentrations. Direct comparison of the TEMPOL and experimental spectrum at high temperatures was not possible because of thermal degradation of the TEMPOL.

EPR spectrum simulations were carried out using a program which simulates the isotropic EPR spectra of up to 10 species with differing *g*-values, concentrations, splittings and line widths.

Density Functional Theory based calculations were performed using the Spartan '02 suite of programs.²⁵ The B3LYP functional and a 6-31G(d) basis set were employed. DFT calculations have been shown to be an appropriate tool to study hydrogen-abstraction reactions. Alkane-*tert*-butoxyl radical complexes were energy minimized while the H(alkane)-

O(*t*-BuO[•]) distance was varied stepwise by applying a distance constraint. In this way, potential energy profiles for H-transfer from alkane to *t*-BuO[•] were obtained. Energy barriers were obtained by subtracting the energy of the weakly-bonded van-der-Waals-type complex from the energy of the complex in the transition state. Temperature-dependent contributions, including both entropy and the entropy-dependent contribution to the enthalpy, were obtained from full vibrational analyses carried out for both the van-der-Waals-type and the transition-state complexes. BDE's, were calculated using the Gaussian98 program,²⁶ also again using the B3LYP functional in conjunction with a 6-31G(d) basis set.

References

- 1 C. Rüchardt, *Angew. Chem. Int. Ed. Engl.*, 1970, **19**, 830.
- 2 J. E. Bennett, B. C. Gilbert, S. Lawrence, A. C. Whitwood and A. J. Holmes, *J. Chem. Soc., Perkin Trans. 2*, 1996, 1789.
- 3 B. C. Gilbert, J. R. Lindsay Smith, P. Taylor, S. Ward and A. C. Whitwood, *J. Chem. Soc., Perkin Trans. 2*, 1999, 1631; B. C. Gilbert, J. R. Lindsay Smith, P. Taylor, S. Ward and A. C. Whitwood, *J. Chem. Soc., Perkin Trans. 2*, 2000, 2001.
- 4 W. Zhou and S. Zhu, *Ind. Eng. Chem. Res.*, 1997, **36**, 1130; T. Yamazaki and T. Seguchi, *J. Polym. Sci., Part A: Polym. Chem.*, 1997, **35**, 279; W. Zhou and S. Zhu, *Macromolecules*, 1998, **31**, 4335; Q. Yu and S. Zhu, *Polymer*, 1999, **40**, 2961; T. Yamazaki and T. Seguchi, *J. Polym. Sci., Part A: Polym. Chem.*, 2000, **38**, 3383.
- 5 T. C. Chung, *Functionalization of Polyolefins*, Academic Press, London, 2002; M. Xantos, *Reactive Extrusion-principles and practise*, Hanser Publisher, Munich, 1992.
- 6 D. G. Hendry, T. Mill, L. Pisskiewicz, J. A. Howard and H. K. Eigenmann, *J. Phys. Chem. Ref. Data*, 1974, **3**(4), 937.
- 7 C. Walling and B. B. Jacknow, *J. Am. Chem. Soc.*, 1960, **82**, 6108.
- 8 E. Niki, N. Ohto, T. Kanauchi and Y. Kamiya, *Eur. Poly. J.*, 1980, **16**, 559.
- 9 P. Dokolas, S. M. Loffler and D. H. Solomon, *Aust. J. Chem.*, 1998, **51**, 1113.
- 10 P. Dokolas, M. G. Looney, S. Musgrave, S. Poon and D. H. Solomon, *Polymer*, 2000, **41**, 3137.
- 11 K. Tominaga, S. Yamauchi and N. Hirota, *J. Phys. Chem.*, 1991, **95**, 3671.
- 12 A. L. J. Beckwith, *J. Chem. Soc.*, 1962, 2248.
- 13 J. K. Kochi, *Adv. Free Rad. Chem.*, 1975, **5**, 189.
- 14 H. Fischer, *Z. Naturforsch.*, 1965, **20a**, 428.
- 15 P. Neta, *Adv. Phys. Org. Chem.*, 1976, **12**, 223.
- 16 Peroxide datasheet, Akzo-Nobel, *personal communication*.
- 17 e.g. M. Weber and H. Fischer, *J. Am. Chem. Soc.*, 1999, **121**, 7381.
- 18 S. Terabe and R. Konaka, *J. Chem. Soc., Perkin Trans. 2*, 1973, 369.
- 19 B. C. Gilbert and M. Trenwith, *J. Chem. Soc., Perkin Trans. 2*, 1973, 1834; P. Franchi, M. Lucarini, G. F. Pedulli and E. Bandini, *Chem. Commun.*, 2002, 560.
- 20 S. Camara, B. C. Gilbert, R. J. Meier, M. van Duin and A. C. Whitwood, work in progress.
- 21 E. Bascetta, F. D. Gunstone and J. C. Walton, *J. Chem. Soc., Perkin Trans. 2*, 1983, 603.
- 22 H. Paul, R. D. Small Jr. and J. C. Scaiano, *J. Am. Chem. Soc.*, 1978, **100**, 4520.
- 23 V. Malatesta and K. U. Ingold, *J. Am. Chem. Soc.*, 1981, **103**, 609.
- 24 A. A. Fokin and P. R. Schreiner, *Chem. Rev.*, 2002, **102**, 1551.
- 25 PC SPARTAN plus is available from Wavefunction Inc., 18401 Von Karman, Suite 370, Irvine, CA 92612, USA (pcsales@wavefun.com; <http://www.wavefun.com>).
- 26 Gaussian 98, Revision A.6 M. J. Frisch, G. W. Trucks, H. B. Schlegel, G. E. Scuseria, M. A. Robb, J. R. Cheeseman, V. G. Zakrzewski, J. A. Montgomery Jr., R. E. Stratmann, J. C. Burant, S. Dapprich, J. M. Millam, A. D. Daniels, K. N. Kudin, M. C. Strain, O. Farkas, J. Tomasi, V. Barone, M. Cossi, R. Cammi, B. Mennucci, C. Pomelli, C. Adamo, S. Clifford, J. Ochterski, G. A. Petersson, P. Y. Ayala, Q. Cui, K. Morokuma, D. K. Malick, A. D. Rabuck, K. Raghavachari, J. B. Foresman, J. Cioslowski, J. V. Ortiz, B. B. Stefanov, G. Liu, A. Liashenko, P. Piskorz, I. Komaromi, R. Gomperts, R. L. Martin, D. J. Fox, T. Keith, M. A. Al Laham, C. Y. Peng, A. Nanayakkara, C. Gonzalez, M. Challacombe, P. M. W. Gill, B. Johnson, W. Chen, M. W. Wong, J. L. Andres, C. Gonzalez, M. Head Gordon, E. S. Replogle and J. A. Pople, Gaussian, Inc., Pittsburgh PA, 1998.